J. Plasma Physics (2006), *vol.* 72, *part* 6, *pp.* 935–939. © 2006 Cambridge University Press
doi:10.1017/S0022377806005332 Printed in the United Kingdom

Parametric study of the resonant scattering process by narrow band whistler mode waves driven by temperature anisotropy

YUTO KATOH and YOSHIHARU OMURA

Research Institute for Sustainable Humanosphere, Kyoto University, Kyoto 611-0011, Japan

(Received 15 August 2005 and accepted 10 January 2006)

Abstract. We study a combined effect of wave trapping due to oppositely propagating narrow band whistler mode waves and discuss its dependence on the background plasma density. In the case where forward and backward traveling whistler mode waves coexist, rapid scattering of resonant electrons occurs owing to the overlapping of diffusion curves of both waves. Simulation results show that the low-density plasma condition, where the electron plasma frequency is close to the electron gyrofrequency, is favorable for the significant resonant scattering of high energetic electrons. The results of the present study suggest that the combined effect plays an important role in energizing relativistic electrons in the equatorial region of the Earth's inner magnetosphere during the recovery phase of geomagnetic storms.

1. Introduction

In recent years, the response of the Earth's outer radiation belt to a geomagnetic storm has been recognized as one of the important subjects of space weather. Results of *in situ* observations have revealed that the flux of relativistic electrons in the outer radiation belt decreases in the main phase and increases again during the recovery phase of a geomagnetic storm (see, for example, Friedel et al. (2002) and references therein). Theoretical analyses have suggested that the resonant scattering process due to whistler mode waves plays a significant role in the energizing process of relativistic electrons (e.g. Summers et al. 1998).

In Katoh and Omura (2004), we reported a combined effect of nonlinear trapping under a condition where oppositely propagating narrow band whistler mode waves coexist due to an instability driven by temperature anisotropy. In the present study, to discuss parameter dependence of the combined effect on the background plasma density (i.e. the ratio of the electron plasma frequency to the electron gyrofrequency), we carried out particle simulation by using the electron hybrid model.

2. Simulation model

We use the model which treats cold electrons as a fluid and hot electrons as particles. The details of the electron hybrid model are described in Katoh et al. (2005). By using a fluid approximation, we can reduce computational costs to solve

https://doi.org/10.1017/S0022377806005332 Published online by Cambridge University Press

Table 1. Initial parameters of the electron species 1 and 2, and estimated maximum growth rate of a whistler mode wave driven by temperature anisotropy. N_1 and N_2 represent the density of the electron species 1 and 2, respectively.

	Π_e/Ω_e	N_2/N_1	$v_{th,\parallel}/c$	$v_{th,\perp}/c$	ω/Ω_e	γ_{max}/Ω_e
Run 1	1.0	1.0×10^{-2}	0.19	0.6	0.615	5.97×10^{-3}
Run 2	2.0	5.0×10^{-3}	0.1	0.4	0.616	5.74×10^{-3}
Run 3	3.0	5.0×10^{-3}	0.05	0.2	0.618	5.78×10^{-3}
Run 4	4.0	4.7×10^{-3}	0.035	0.14	0.611	5.83×10^{-3}

gyromotions of cold electrons taking into account the dispersive nature of cold plasma medium. We use a periodic, one-dimensional simulation system and assume three electron species as follows. The background cold electrons, we refer to as species 1, are treated as a fluid and their motions are solved by the fluid equation of motion, whereas both electron species 2 and 3 are treated as particles including fully relativistic effects.

In this paper we present four simulation results under different initial conditions given in Table 1. In each simulation run, we assume that the electron species 2 has a temperature anisotropy which generates narrow band whistler mode waves. We select both the temperature anisotropy of the initial distribution and the density ratio of the species 2 to background plasma so that the same growth rate of whistler mode waves is achieved as shown in Fig. 1(a). Since the instability is rapidly quenched by the relaxation of the anisotropy, we apply recycling of particles (Dum 1985) to the electron species 2. A small fraction of the particles are initialized at every time step. At every cycle of $225\Omega_e^{-1}$, whole particles of the electron species 2 are eventually replaced. To see the basic process of the combined effect of oppositely propagating waves, the distribution function of the species 3 of electrons is assumed to be a ring distribution defined in the momentum space given by

$$f(u_\parallel, u_\perp) = C \exp\left[-\frac{(u_\parallel - u_{d\parallel})^2 + (u_\perp - u_{d\perp})^2}{u_a^2}\right],$$

where $u_\parallel$ and $u_\perp$ denote a parallel and a perpendicular component of momentum to the magnetic field direction, respectively, and C is a constant. We assume $u_{d\parallel} = 0$, $u_{d\perp} = 1.5c$ and $u_a = 5\times10^{-2}c$, and that the density ratio of the species 3 to background plasma is 10^{-6}.

3. Simulation results

In each simulation run, oppositely propagating whistler mode waves are self-consistently excited while frequencies of both whistler mode waves are naturally the same. Figures 2(a)–(d) show the distribution of the electron species 3 in the momentum space at $1800\Omega_e^{-1}$. We also present diffusion curves of oppositely propagating whistler mode waves with a frequency band width from $0.4\Omega_e$ to $0.8\Omega_e$. The overlapping of the diffusion curves causes rapid resonant scattering of electrons of species 3, as shown in Fig. 2. The simulation results suggest that the efficient resonant scattering occurs in the case of the low-density background plasma condition. Indeed, the maximum acceleration rate of resonant electrons is 48% in Run 1 (some selected electrons are accelerated from 365 to 540 keV during $1800\Omega_e^{-1}$), whereas it is 4% in Run 4.

https://doi.org/10.1017/S0022377806005332 Published online by Cambridge University Press

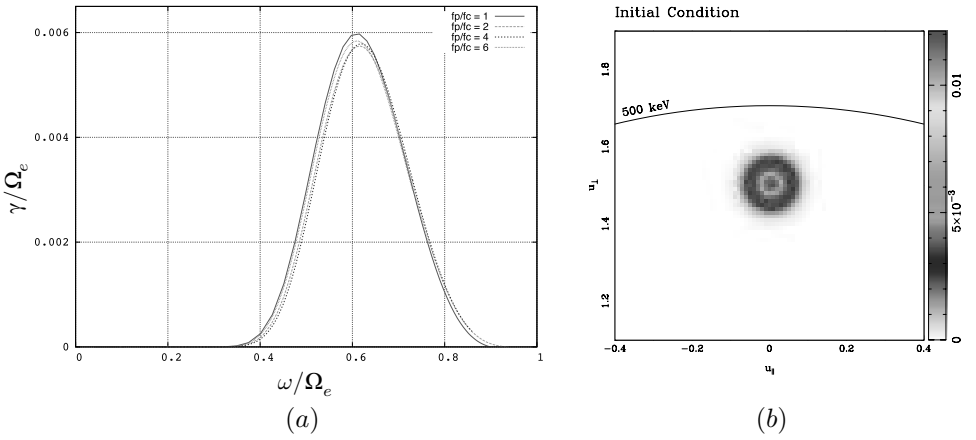


Figure 1. (a) Linear growth rate of whistler mode waves. (b) Initial distribution of the electron species 3.

This dependency on the background plasma density is explained by the characteristics of the whistler mode wave. Under the background plasma condition assumed in Run 1, the phase velocity of whistler mode wave becomes larger than that in Run 4; the phase velocity of the whistler mode wave with the frequency of $0.6\Omega_e$ is $0.44c$ in Run 1, whereas it is $0.08c$ in Run 4. Due to the large phase velocity, since diffusion curves of whistler mode waves are steepened against the constant energy line, significant energy diffusion of resonant electrons are induced in Run 1. Moreover, in the case where the amplitude of excited whistler mode waves is at the same level in each simulation run, the small wavenumber k of whistler mode waves in the condition of Run 1 results in a large trapping velocity $v_T = 2\sqrt{v_\perp \Omega_W / k}$, where $\Omega_W = eB_W/m_e$ and B_W is the amplitude of the wave magnetic field. Since the effect of nonlinear trapping is estimated by the trapping velocity, the combined effect observed in Run 1 is significantly enhanced by the nonlinear trapping; resonant electrons are effectively scattered within the overlapping region of diffusion curves as shown in Fig. 2(a).

4. Summary and discussions

Results of *in situ* observations in the equatorial region of the inner magnetosphere show that energetic electrons often have an anisotropic velocity distribution during a geomagnetic storm. Since the temperature anisotropy drives the instability generating oppositely traveling narrow band whistler mode waves, the combined effect of oppositely propagating whistler mode waves studied in the present paper plays an important role in the storm-time energizing of relativistic electrons.

In the present study, we have shown the efficiency of the combined effect depends critically on the ratio of the electron plasma frequency to the electron gyrofrequency, Π_e/Ω_e; a smaller ratio is favorable for rapid scattering of resonant electrons. This result is consistent with observations that the flux increase of radiation-belt electrons occurs at the outside region of the plasmapause where the ratio is typically less than four (Horne et al. 2005).

https://doi.org/10.1017/S0022377806005332 Published online by Cambridge University Press

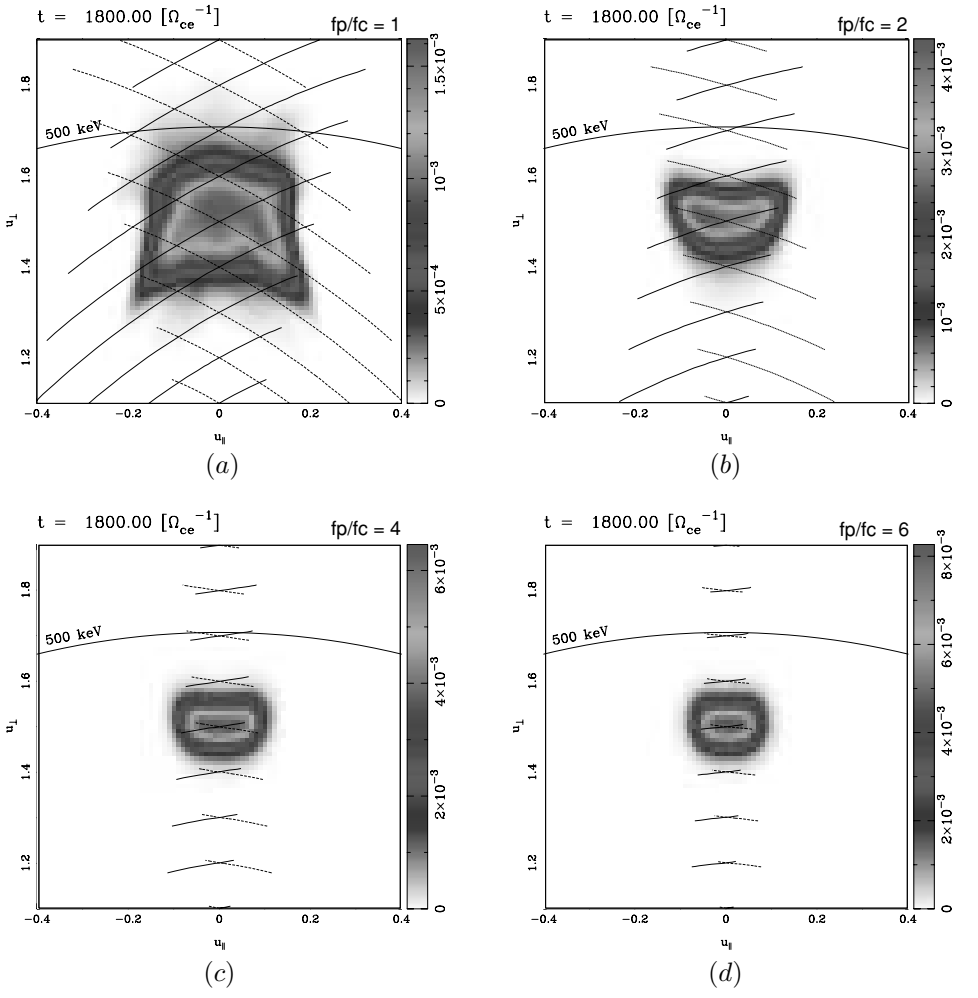


Figure 2. Distribution of the electron species 3 at 1800 Ω_e^{-1} in (a) Run 1, (b) Run 2, (c) Run 3 and (d) Run 4. We also represent diffusion curves of both forward (solid curve) and backward (dashed curve) propagating whistler mode waves.

Finally, we should note that the physics appearing in the present simulation corresponds to the phenomena in the equatorial region of the Earth's inner magnetosphere. The combined effect discussed in the present study should be suppressed by the mirror force due to the spatial inhomogeneity of geomagnetic field, because the resonant interaction time should be shorter than that at the equatorial region. Therefore, the combined effect should take place only around the magnetic equator where magnetic inhomogeneity is relatively small. The effect of semi-inhomogeneous magnetic field on the resonant scattering process should be examined in future studies.

Acknowledgements

Computation in the present study was performed with the KDK system of RISH at Kyoto University. This work was partially supported by Kyoto University

https://doi.org/10.1017/S0022377806005332 Published online by Cambridge University Press

Active Geosphere Investigations for the 21st Century Centers of Excellence Program (KAGI21).

References

Dum, C. T. 1985 In: *Computer Simulation of Space Plasmas* (eds H. Matsumoto and T. Sato), p. 303. Tokyo: Terra Scientific.

Friedel, R. H. W., Reeves, G. D. and Obara, T. 2002 *J. Atmos. Sol.–Terr. Phys.* **64**, 265–282.

Horne, R. B. et al. 2005 *J. Geophys. Res.* **110**, A03225. doi:10.1029/2004JA010811.

Katoh, Y. and Omura, Y. 2004 *J. Geophys. Res.* **109**, A12214. doi:10.1029/2004JA010654.

Katoh, Y., Ono, T. and Iizima, M. 2005 In: *The Inner Magnetosphere: Physics and Modeling* (eds T. Pulkkinen, R. H. W. Friedel and N. Tsyganenko), Geophys. Monograph Series 155, pp. 33–39 AGU, Washington, DC.

Summers, D., Thorne, R. M. and Xiao, F. 1998 *J. Geophys. Res.* **103**, 20 487–20 500.

https://doi.org/10.1017/S0022377806005332 Published online by Cambridge University Press